J. Fluid Mech. (1982), *vol.* 123, *pp.* 425–442
Printed in Great Britain

Wind-induced growth of water waves

By H. MITSUYASU AND T. HONDA
Research Institute for Applied Mechanics, Kyushu University, Fukuoka 812, Japan

(Received 13 November 1981 and in revised form 5 May 1982)

Spatial growth of mechanically generated water waves under the action of wind has been measured in a laboratory wind-wave flume both for pure water and for water containing a surfactant (sodium lauryl sulphate, concentration $2{\cdot}6 \times 10^{-2}\%$). In the latter case, no wind waves develop on the surface of the mechanically generated waves as well as on the still water surface for wind speeds up to $U_{10} \approx 15$ m/s, where U_{10} is the wind velocity at the height $Z = 10$ m. Therefore we can study the wind-induced growth of monochromatic waves without the effects of co-existing short wind waves. The mechanically generated waves grew exponentially under the action of the wind, with fetch in both cases. The measured growth rate β for the pure water can be fitted by $\beta/f = 0{\cdot}34\,(U_*/C)^2$, $0{\cdot}1 \lesssim U_*/C \lesssim 1{\cdot}0$, where f is the frequency of the waves, C is the corresponding phase velocity, and U_* is the friction velocity obtained from vertical wind profiles. The effect of the wave steepness H/L on the dimensionless growth rate β/f is not clear, but seems to be small. For water containing the surfactant, the measured growth rate is smaller than that for pure water, but the friction velocity of the wind is also small, and the above relation between β/f and U_*/C holds approximately if the measured friction velocity U_* is used for the relation.

1. Introduction

During the last twenty years, there has been a great progress in various aspects of the wind-wave problem. However, there still remain important aspects that are poorly understood. One of the central problems is the growth mechanism of wind waves, which is very difficult to clarify not only theoretically but also experimentally. The experimental difficulty of this problem arises from the following reasons.

The evolution of the power spectrum $\Psi(\omega; x, t)$ of the wind wave is governed by an energy balance equation (Hasselmann 1968)

$$\frac{\partial \Psi}{\partial t} + C_g \frac{\partial \Psi}{\partial x} = S_{in} + S_{nl} + S_{ds}, \tag{1}$$

where C_g is the group velocity, S_{in} is the energy input from the wind, S_{nl} is the nonlinear energy transfer due to wave–wave interaction, and S_{ds} is the energy dissipation. Therefore, measurements of $\partial\Psi/\partial x$ do not give direct information on S_{in}. On the other hand, direct measurement of S_{in} is very difficult technically, and accurate data of S_{in} are still limited (Dobson 1971; Elliott 1972; Snyder *et al.* 1981).

In order to overcome the difficulties and to clarify the growth mechanism of wind waves, a study of the growth of mechanically generated waves under wind action seems to be a powerful approach, at least as a first step, because we are free of the difficult problem of nonlinear wave–wave interaction among spectral components (Hasselmann 1968). In fact, several studies have been made along this line, though

the experimental conditions are still limited (Bole & Hsu 1969; Gottifredi & Jameson 1970; Wilson *et al.* 1973; Mizuno 1975). Even in this approach, however, the problem is not so simple as we expect. That is, when the wind blows over the mechanically generated waves, the waves are superimposed by wind-generated short waves. Here again we encounter complicated problems of the interaction between long and short water waves such as those studied by Phillips (1963), Mitsuyasu (1966), Longuet-Higgins (1969), Hasselmann (1971), Phillips & Banner (1974), Garrett & Smith (1976), Valenzuela & Wright (1976), and Hatori, Tokuda & Toba (1981). The use of a surfactant in the experiment much simplifies the problem, because wind waves do not develop on the mechanically generated waves up to fairly high wind speeds. Therefore, in the present study, the growth of mechanically generated water waves under wind action is measured both for pure water (tap water) and for water containing surfactant. We examine, in the former case, the growth of regular waves co-existing with short wind waves, and in the latter case, the growth of regular waves unaffected by wind waves. By comparing the results of these two measurements, we clarify the effects of short wind waves on the growth of the longer waves.

2. Equipment and procedure

2.1. *The wind-wave flume*

The experiment was carried out in a wind-wave flume 0·8 m high, 0·6 m wide and with a usual test-section length of 15 m. Water depth in the flume was kept at 0·335 m throughout the experiment. The arrangement of the equipment is shown schematically in figure 1. A beach for absorbing wave energy and a centrifugal fan for sucking air through the flume were situated downwind of the test section (outside right of figure 1). At the upwind side, the air was carried on to the water surface by an elbow that contained turning vanes, honeycombs, a screen and a transition plate. A flap-type wave generator at the upwind side was used for generating regular oscillatory waves.

The periods of the regular waves were $T = 0{\cdot}6$, 0·7, 0·8, 1·0, 1·3 (s), and their steepnesses were in the range $\delta = 0{\cdot}01$–$0{\cdot}06$. For each wave with a different period, the wave steepness was changed successively as 0·01, 0·02, ..., 0·06, within a range where the generation of stable regular waves is possible. Some of the short waves with large steepness were unstable and showed three-dimensional instability. These waves were eliminated from the test waves.† The waves were measured simultaneously at eleven stations with resistance-type wave gauges.

Wind speed U_r in the flume was changed stepwise as $U_r = 5$, 7·5, 10, 12·5 (m/s),

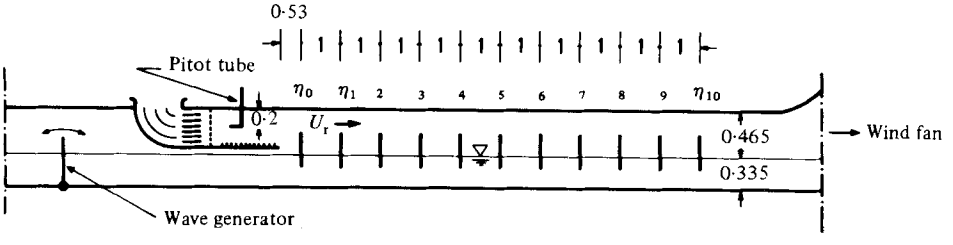

FIGURE 1. Schematic diagram of wind-wave flume (units in m).

† However, it is inevitable that some waves of relatively large steepness become unstable after a period of wind-induced growth.

Experiment no.	$C_{12}H_{25}O\ SO_4Na$ Mass (g)	$C_{12}H_{25}O\ SO_4Na$ Concentration %	ν_w (cSt)	γ (dyn/cm)
I	0	Tap water	1·8	74
	70	$2{\cdot}3 \times 10^{-3}$	1·7	64
	150	$5{\cdot}0 \times 10^{-3}$	1·6	49
	220	$7{\cdot}3 \times 10^{-3}$	1·6	42
	790	$2{\cdot}6 \times 10^{-2}$	1·6	28
II	0	Tap water	1·8	75
	790	$2{\cdot}6 \times 10^{-2}$	1·8	27
III	0	Tap water	1·6	70
	790	$2{\cdot}6 \times 10^{-2}$	1·6	27

TABLE 1. Data on the water with or without the surfactant $C_{12}H_{25}O\ SO_4Na$: ν_w is kinematic viscosity, γ is surface tension. The experiments took several days. The values of ν_w and γ changed slightly in each day. Therefore, mean values are shown in the table.

and monitored with a Pitot static tube installed above the transition plate. Here, the wind speed U_r corresponds roughly to a cross-sectional mean speed after the correction of a small change in the cross-sectional area. Vertical wind profiles over the water surface were measured with another Pitot static tube at fetches X = 1·85, 3·03, 4·26, 5·49, 6·72, 9·15, 10·62, 12·09 (m).

2.2. *Materials*

Almost the same measurements were repeated using pure water (tap water) and water containing a surfactant (sodium lauryl sulphate, $C_{12}H_{25}OSO_3Na$) with concentration $2{\cdot}6 \times 10^{-2}$ %. In the latter case wind waves were almost completely suppressed up to the wind speed U_r = 10 m/s ($U_* \approx 45$ cm/s). Therefore the growth of the regular waves under the action of the wind is measured without the effect of wind-generated waves. The properties of the water were measured before and after each experiment. The data on the water without or with the surfactant are shown in table 1.

2.3. *Experimental procedure*

Before the wave-growth experiment described below, regular waves generated by the wave generator were measured at 11 stations without the wind, and wave-attenuation data were obtained. The wave-attenuation data were used later to determine a net growth rate of regular waves under the action of the wind by compensating for the effect of viscous energy dissipation.

In the wave-growth experiment, wind waves were generated first in the test section by wind of a prescribed speed. After the time when the wind waves had attained a stationary state, the wave generator was operated and a regular oscillatory wave with given properties was made to propagate through the wind-generated wave field in the test section. After the start of the wind, waves were continuously measured at 11 stations and recorded on a TEAC-280 FM data recorder. Therefore, the initial part of the wave record contains wind waves in transient and steady states, and the later part contains a co-existent system of wind waves and the regular waves. In the present study, the later part of the data is mainly studied. For the water containing the surfactant, no wind waves were generated by the wind. However, the same procedure as described above was used in the measurement.

3. Analysis of the wave data

The wave records of each run were digitized at a sampling frequency of approximately 100 Hz. Strictly speaking, the sampling frequency was changed slightly, depending on the period of regular waves, so that the duration of 2048 sampled data becomes an integral multiple of each wave period. This procedure is required to reduce the leakage effect of the spectral density, because we intend to study line spectra for the fundamental component of the regular waves. Power spectra of waves were computed through a fast-Fourier-transform procedure using each 2048-point data set. Seven samples of the spectral data were obtained for each run and the sample mean of the spectra was used for further analysis. As expected, the leakage effect of the fundamental component of the regular waves was negligibly small. Therefore we used a sum of the fundamental line spectrum and its adjacent line spectra in both sides as a spectral energy of the fundamental component, though the latter were much smaller than the former (less than 10 %). Throughout the present study, the spectral density of the fundamental component obtained by the above procedure is analysed and its attenuation or growth by the wind is studied.

4. Results

4.1. *Wind profile over the water surface*

Vertical wind profiles $U(z)$ were measured both for pure water and for water containing surfactant. In the latter case no wind waves were generated up to the wind speed $U_r = 10$ m/s. As shown in figure 2, the wind profiles over the water surface contaminated by the surfactant differ from those over the clean water surface, though both profiles show the logarithmic distribution,

$$U(z) = \frac{U_*}{\kappa} \ln \frac{Z}{Z_0}, \tag{2}$$

where $U_* \equiv (\tau_s/\rho_a)^{\frac{1}{2}}$, ($\tau_s$ is the wind shear stress, ρ_a is the density of the air) is the friction velocity of the wind, κ is Kármán's constant ($\approx 0{\cdot}4$), and Z_0 is a roughness parameter of the water surface. The values of U_* and Z_0 were determined from the measured wind profile $U(z)$ by fitting the logarithmic distribution (2). Furthermore, the wind speed U_{10} at the height $Z = 10$ m was determined by extrapolation of the logarithmic distribution (2). The friction velocity U_* thus determined is used for the analysis of wave-growth data. The details of the wind measurements will be published elsewhere (Mitsuyasu & Honda 1982) and only typical examples of the data are shown in table 2.

4.2. *Attenuation of regular waves*

In our experimental conditions, the change of the spectral energy E of the regular waves under wind action is given by

$$C_g \frac{\partial E}{\partial x} = S_{in} + S_{nl} + S_{ds}, \tag{3}$$

where C_g is the group velocity of the regular waves, S_{in} is the energy input from the wind, S_{nl} is the nonlinear energy transfer due to the interaction between the regular waves and co-existing wind waves, and S_{ds} is the energy dissipation. In order to determine S_{in} or $S_{in} + S_{nl}$ from the measured value of $C_g\, \partial E/\partial x$ we need to determine

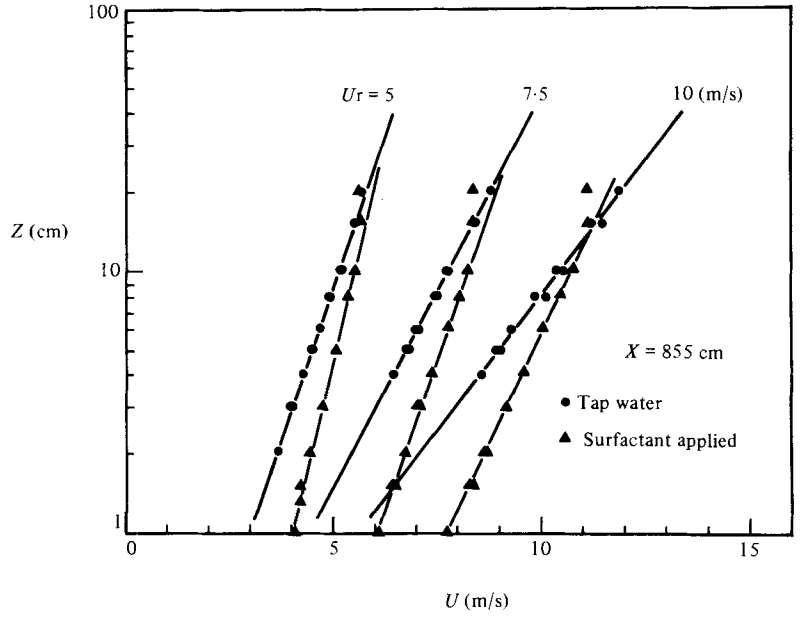

FIGURE 2. Wind profiles over the water surface.

U_r (m/s)	U_{10} (m/s)	U_* (cm/s)	Z_0 ($\times 10^{-3}$ cm)	Remarks
5·0	6·9	22·4	4·3	Tap water
7·5	10·8	35·8	6·0	X = 5·49 m
10·0	15·1	54·1	14	
12·5	24·6	116	208	X = 6·72 m
5·0	7·3	21·5	1·2	Surfactant
7·5	11·1	31·2	0·7	($2{\cdot}6 \times 10^{-2}$%)
10·0	14·9	43·5	1·2	X = 6·72 m
11·4	17·8	53·7	1·8	

TABLE 2. Wind data

S_{ds} separately. In other words, in order to determine the net growth rate of the regular waves by the wind we need to correct the measured growth rate by taking account of the energy dissipation. For this purpose, we first studied the attenuation of the regular waves with no wind.†

Results for pure water. Figure 3 shows the change of the spectral energy E of the fundamental frequency component of regular waves propagating on the pure water with no wind. A damping coefficient Δ was determined from the data of E by fitting the relation

$$E = E_0 \exp(-\Delta x), \tag{4}$$

which is shown by straight lines in figure 3.

† Although the energy dissipation of the regular waves under the action of the wind may differ slightly from that in the absence of the wind, we have no way to determine it directly from the wave data measured under the action of the wind.

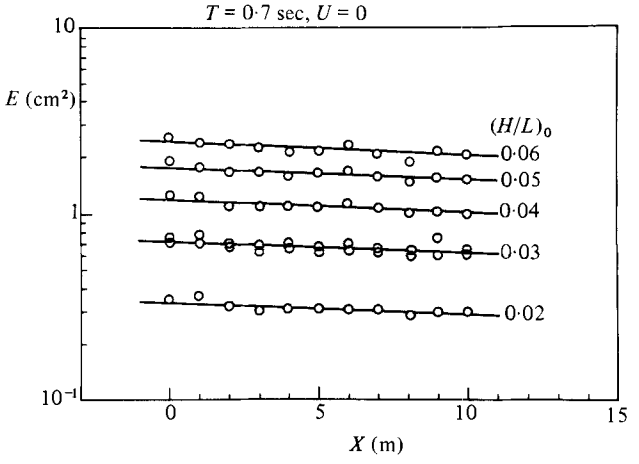

FIGURE 3. Plot of E versus x for tap water in the absence of wind.

H/L \ T	0·6 s	0·7 s	0·8 s	1·0 s	1·3 s
0·01	—	—	—	—	$1{\cdot}14\times10^{-4}$
0·02	$2{\cdot}03\times10^{-4}$	$1{\cdot}55\times10^{-4}$	$1{\cdot}39\times10^{-4}$	$1{\cdot}24\times10^{-4}$	$1{\cdot}14\times10^{-4}$
0·03	$2{\cdot}06\times10^{-4}$	$1{\cdot}59\times10^{-4}$	$1{\cdot}43\times10^{-4}$	$1{\cdot}25\times10^{-4}$	$1{\cdot}18\times10^{-4}$
0·04	$2{\cdot}08\times10^{-4}$	$1{\cdot}59\times10^{-4}$	$1{\cdot}49\times10^{-4}$	—	—
0·05	$2{\cdot}16\times10^{-4}$	$1{\cdot}66\times10^{-4}$	$1{\cdot}52\times10^{-4}$	—	—
0·06	$2{\cdot}10\times10^{-4}$	$1{\cdot}65\times10^{-4}$	$1{\cdot}53\times10^{-4}$	—	—
Mean	$2{\cdot}09\times10^{-4}$	$1{\cdot}61\times10^{-4}$	$1{\cdot}47\times10^{-4}$	$1{\cdot}25\times10^{-4}$	$1{\cdot}15\times10^{-4}$
Theory†	$2{\cdot}38\times10^{-4}$	$1{\cdot}83\times10^{-4}$	$1{\cdot}48\times10^{-4}$	$1{\cdot}11\times10^{-4}$	$0{\cdot}86\times10^{-4}$

† Kinematic viscosity of water is taken as $\nu = 0{\cdot}018$

TABLE 3. Exponential decay rate Δ; $E = E_0\exp(-\Delta x)$.

The experimental values of Δ are summarized in table 3, and compared with the theoretical values of Δ due to the viscous dissipation, which were determined by

$$\Delta = \Delta_s + \Delta_b. \tag{5}$$

Here Δ_s is the surface damping coefficient (Lamb 1932),

$$\Delta_s = 16\nu k^2 \frac{\omega}{g}\frac{\cosh^2 kd}{\sinh 2kd + 2kd}, \tag{6}$$

where ν is the kinematic viscosity of the water, $k = 2\pi/L$ is the wavenumber, ω is the angular frequency, g is the gravitational acceleration, and d is the water depth in the flume.

The second term Δ_b is the damping coefficient due to boundary dissipation at side walls and a bottom of the flume, which is given by (Hunt, 1952)

$$\Delta_b = \frac{4k}{b}\left(\frac{\nu}{2\omega}\right)^{\frac{1}{2}}\frac{kb + \sinh 2kd}{\sinh 2kd + 2kd}, \tag{7}$$

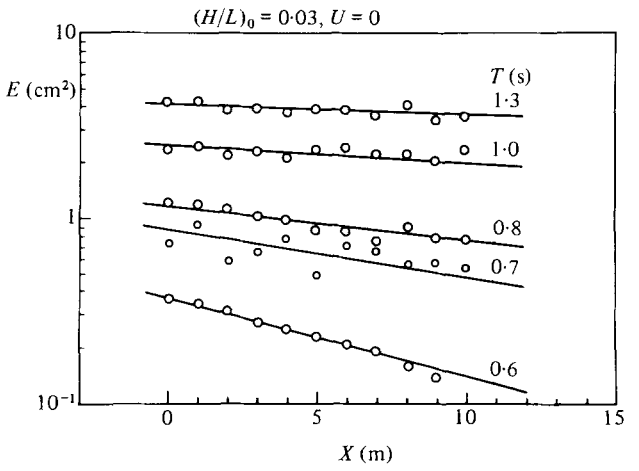

FIGURE 4. The same as figure 3 except for water containing the surfactant (concentration $2{\cdot}6 \times 10^{-2}$ %).

where b is the width of the flume. From table 3 one sees that measured values of Δ agree fairly well with the theoretical values, though the former depend weakly on the wave steepness.

Results for the water containing the surfactant. Figure 4 shows the change of E for regular waves propagating on the water containing surfactant. In this case, the energy dissipation increases owing to the effect of the surface film of surfactant. The straight lines in figure 4 were determined by taking account of the surface dissipation due to the immobile surface film and the boundary dissipation previously discussed. The surface damping coefficient due to an immobile surface (Lamb, 1932) can be expressed in similar form as

$$(\Delta_s)_{\text{imm}} = \frac{4k}{b}\left(\frac{\nu}{2\omega}\right)^{\frac{1}{2}} \frac{kb \sinh^2 kd}{\sinh 2kd + 2kd}. \tag{8}$$

Figure 4 shows fairly good agreement between the theory and the measurement.

4.3. *Growth of the regular waves by the wind (pure water)*

Figures 5 and 6 show typical records of regular waves under the action of the wind, which were measured at fetches $X = 0$, 3, 6, 9 (m). The fetch X is measured from the location of the first wave gauge. For comparisons, record of wind waves in the absence of the regular waves are shown in the upper side of each record of the regular waves.

Figures 7 and 8 show wave spectra corresponding to the records shown in figures 5 and 6, though the wave spectra at all stations, fetches $X = 0, 1, 2, \ldots, 10$ (m), are shown in these figures. The first sharp spike corresponds to the fundamental frequency component of the regular waves. For the waves of large steepness, higher harmonics can be seen clearly (figure 8), but they are not clear for the waves of small steepness (figure 7). As reported previously (Mitsuyasu 1966; Phillips & Banner 1974), wind-generated waves overlap, with a little attenuation, on the regular waves of small steepness (figures 5 and 7), but they are much suppressed by the regular waves of large steepness (figures 6 and 8). A remarkable increase of the harmonics of the regular waves is seen in the latter case. Even when the steepness of regular waves is initially small, the steepness increases with fetch as the regular waves develop, and wind waves

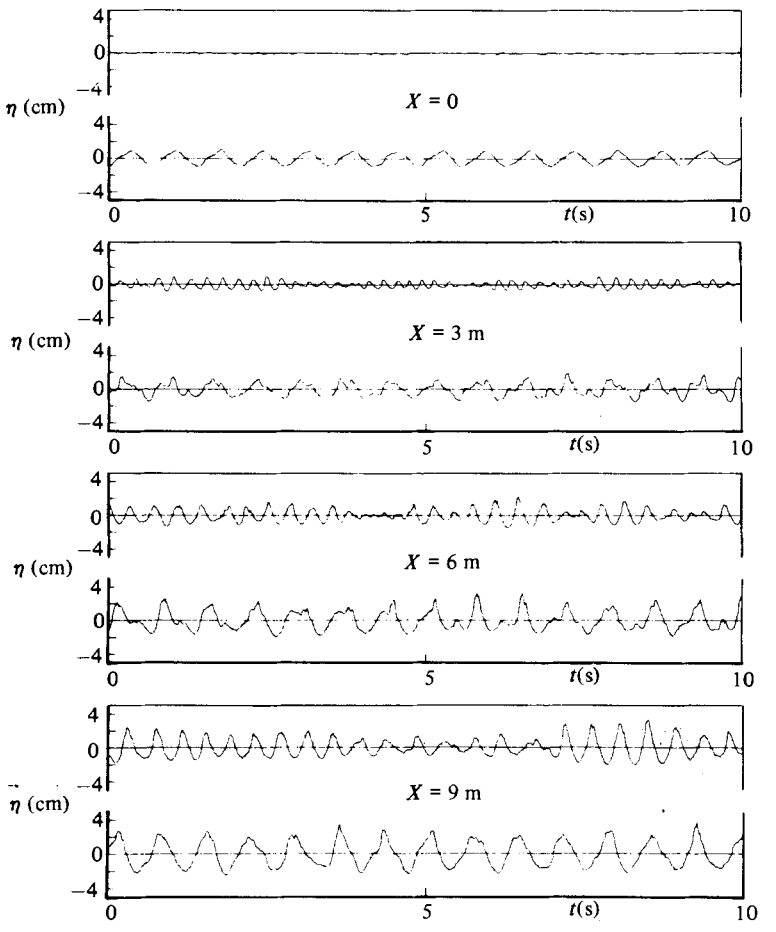

FIGURE 5. Sample records for waves at fetches 0, 3 m, 6 m and 9 m. Upper record is of the wind wave in the absence of the regular waves. Lower record is of the regular waves under the action of the wind ($T = 0{\cdot}7$ s, $(H/L)_0 = 0{\cdot}02$, $U_r = 10$ m/s).

are finally suppressed at large fetch ($X = 9$ m in figure 7). However, our present concern is the wind-induced growth of the regular waves, and we will not enter into further discussions of the wind waves.

4.4. *Growth rate of the regular waves (pure water)*

The spectral energy E of the fundamental frequency component of the regular waves was plotted against the distance x in a log-linear scale. Typical examples of the data are shown in figure 9. Except for a region of very short fetches where the wind shear stress is not uniform owing to a special configuration of the wind-wave flume,† the growth of the fundamental frequency component is exponential. The exponential growth rate α' was determined by fitting the relation

$$E = E_0 \exp \alpha' x \tag{9}$$

to the data at relatively large fetches. Regular waves with large steepness

† There is a gap between the transition plate and the water surface to enable the regular waves to pass through it. This gap introduces a sheltered area over the water surface at short fetch. The first wave gauge is located roughly at the position where the wind jet contacts the water surface.

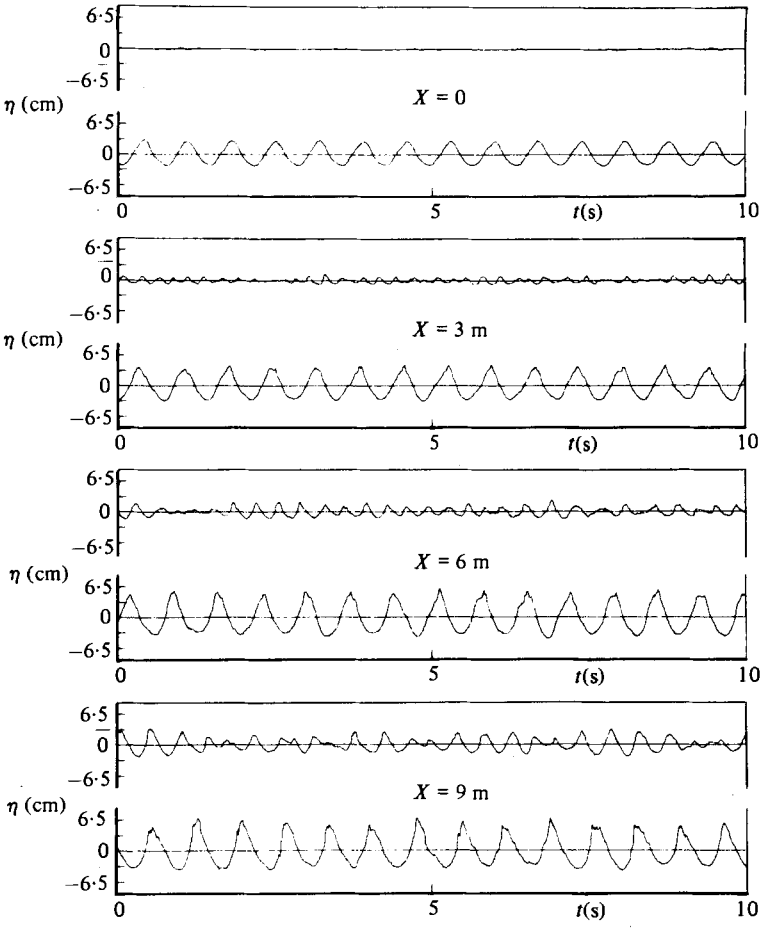

FIGURE 6. The same as figure 5 except for $(H/L)_0 = 0{\cdot}06$.

($(H/L)_0 = 0{\cdot}05$, $0{\cdot}06$), after a period of rapid growth under the action of wind, tend to saturate and break at long fetches. Therefore, a least-square method has been applied to the data before breaking.

As discussed in §4.2, the growth rate α' is affected by the viscous energy dissipation, and a net growth rate α need to be determined by using the equation

$$E = E_0 \exp \alpha' x = E_0 \exp (\alpha - \Delta) x, \tag{10}$$

where Δ is the damping coefficient determined in §4.2. In the present analysis, however, we use another method.

Equation (10) can be rewritten as

$$\frac{E}{(E)_0} = \exp \alpha x, \tag{11}$$

where

$$(E)_0 = E_0 \exp (-\Delta x) \tag{12}$$

is the wave energy affected by the viscous energy dissipation, which corresponds to the original data used in §4.2 for determining the damping coefficient Δ. The data

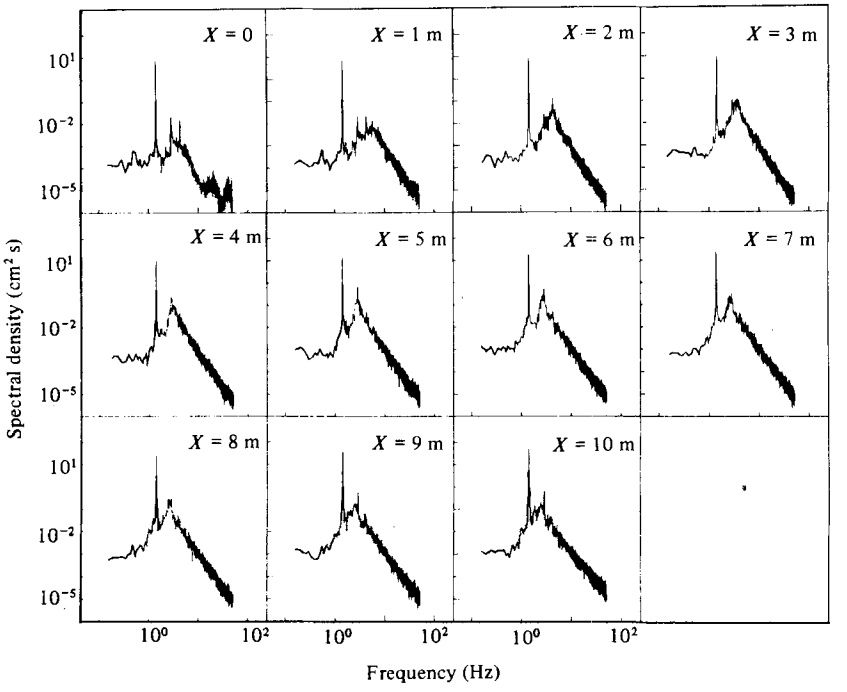

FIGURE 7. Growth of the wave spectrum for tap water (regular wave; $T = 0{\cdot}7$ s, $(H/L)_0 = 0{\cdot}02$; Wind, $U_r = 10$ m/s).

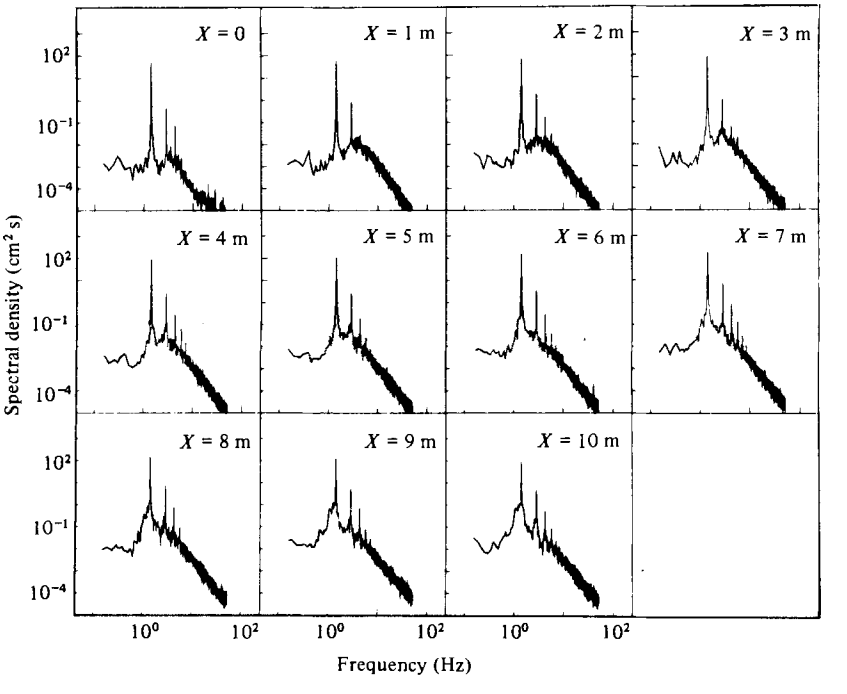

FIGURE 8. The same as figure 7 except for $(H/L)_0 = 0{\cdot}06$.

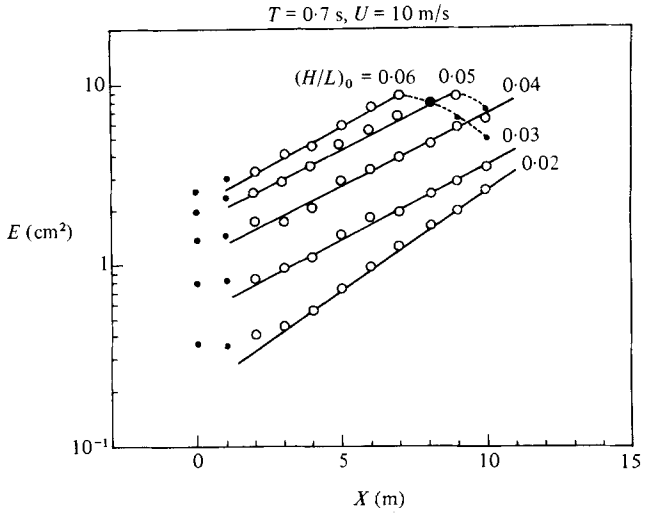

FIGURE 9. Plot of E versus x for tap water under the action of the wind.

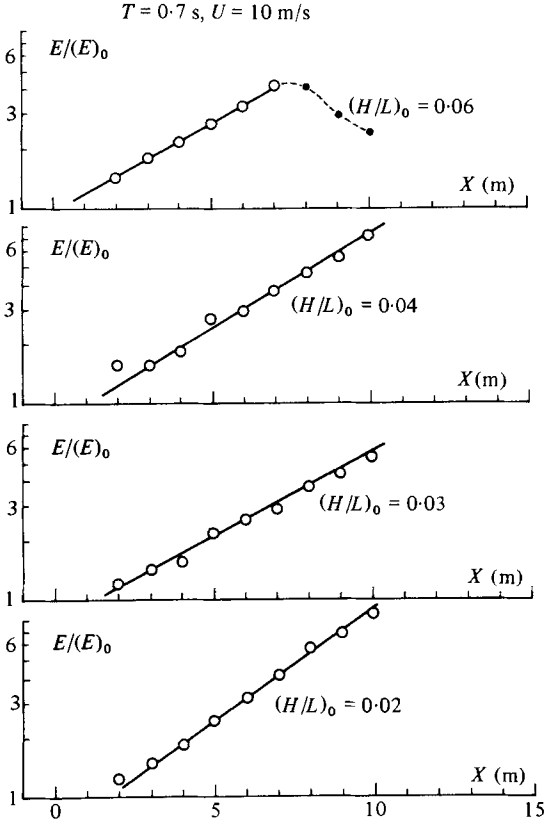

FIGURE 10. Plot of $E/(E)_0$ versus x.

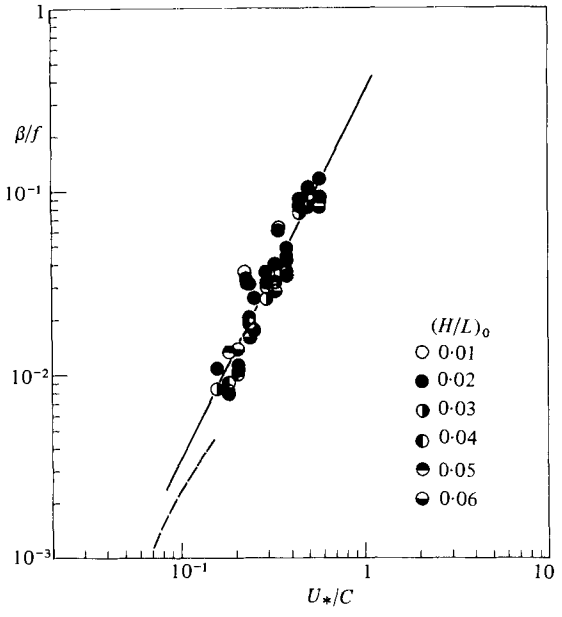

FIGURE 11. Plot of β/f versus U_*/C. The solid line is (14) and the broken line is (18,.

of $E/(E)_0$ were plotted against x (figure 10) and the exponential growth rate α was determined by a least squares method. Here again we eliminated some data of E at very short fetches and long fetches.

The spatial growth rate α thus determined, was converted to the temporal growth rate β through the relation

$$\beta = C_g \alpha, \tag{13}$$

where C_g was determined from linear theory.

Then the relation between the dimensionless growth rate β/f and the dimensionless friction velocity of the wind U_*/C was examined (figure 11), where f is the frequency of the fundamental component of the regular waves and C is the corresponding phase velocity determined from linear theory. Although there is a trend that β/f depends weakly on the initial wave steepness $(H/L)_0$, we neglect the effect of $(H/L)_0$ in the present analysis, because the effect of the initial wave steepness $(H/L)_0$ on the dimensionless growth rate β/f is relatively small, as shown in figure 11.

The best-fit relation for the present data is given by

$$\frac{\beta}{f} = 0{\cdot}34\left(\frac{U_*}{C}\right)^2 \quad \left(0{\cdot}1 \lesssim \frac{U_*}{C} \lesssim 1\right), \tag{14}$$

which is shown in figure 11 by a solid straight line. As shown in the figure, scatter of the data is relatively small.

In order to compare the present relation (14) with those reported previously, typical relations obtained by various authors are shown in figure 12. Included in figure 12 are the following.

(i) The predicted relation arising from the theory of Miles (1959)

$$\frac{\beta}{f} = 2\pi \frac{\beta'}{\kappa^2} \frac{\rho_a}{\rho_w}\left(\frac{U_*}{C}\right)^2 = 0{\cdot}16\left(\frac{U_*}{C}\right)^2, \tag{15}$$

where ρ_w is the density of the water. In the derivation of (15), a dimensionless pressure coefficient β' (β in the notation of Miles 1959) was taken as 3·4, because the wind-profile parameter $\Omega = gZ_0/U_1^2$ was of the order of 2×10^{-3} and C/U_1 was in the range 0·4–4·0 in our experimental condition. Here U_1 is given by $U_1 = U_*/\kappa$.

(ii) The empirical relation from Inoue (1966):

$$\frac{\beta}{f} = \frac{6{\cdot}27}{3600}\left(\frac{U}{C}\right)^2 \exp\left\{-0{\cdot}017\left(\frac{C}{U}\right)^4\right\}$$

$$= 1{\cdot}23\left(\frac{U_*}{C}\right)^2 \exp\left\{-3{\cdot}2 \times 10^{-8}\left(\frac{C}{U_*}\right)^4\right\}. \tag{16}$$

(iii) The empirical relation from Snyder & Cox (1966):

$$\frac{\beta}{f} = 2\pi\frac{\rho_a}{\rho_w}\left\{\frac{U}{C} - 1\right\}$$

$$= 0{\cdot}20\left(\frac{U_*}{C}\right) - 8{\cdot}2 \times 10^{-3}. \tag{17}$$

In the relations (16) and (17), a reference wind speed U is assumed as $U = U_{19{\cdot}5} = 27U_*$, where $U_{19{\cdot}5}$ is the wind speed at the height 19·5 m.

(iv) The empirical relation from Snyder *et al.* (1981):

$$\frac{\beta}{f} = 0{\cdot}04\left(\frac{U_*}{C}\right) - 1{\cdot}7 \times 10^{-3} \quad \left(0{\cdot}05 < \frac{U_*}{C} < 0{\cdot}13\right). \tag{18}$$

This relation is obtained from their original form for the growth-rate parameter $\mathrm{Im}\,\gamma$, $\mathrm{Im}\,\gamma = (0{\cdot}2\text{–}0{\cdot}3)\ (U_5/C - 1)$, using the relation $\beta/f = 2\pi(\rho_a/\rho_w)\,\mathrm{Im}\,\gamma$ and assuming $\rho_a/\rho_w = 1{\cdot}2 \times 10^{-3}$ and $U_5 = 23U_*$. Several field data of β/f and our data are also shown in figure 12, though the same symbol is used for our data irrespective of wave steepness.

Figure 12 shows that our growth rate given by (14) is larger, by a factor of about two, than Miles' (1959) growth rate and a little larger than the growth rate of Snyder *et al.* (1981), but smaller than that of Inoue (1966). The relation (17) from Snyder & Cox (1966) shows a different trend from (14), but an extrapolation of (17) fits fairly well to the present data. The field data of Schule, Simpson & Deleonibus (1971) is fairly close to the present relation (14).

However, it should be noted that the existence of the critical layer in the logarithmic region of the wind profile is questionable in our experimental conditions. Therefore, the application of Miles' (1959) theory is not necessarily adequate, and the disagreement between the theory and the measurement does not mean a failure of the theory. The comparison of the present result with the viscous theory of Miles (1962) may also be inadequate, because the existence of a viscous sublayer is questionable in our experimental conditions.

It should be also mentioned that the relation (18) from Snyder *et al.* (1981) is one of the most reliable relations determined from field data, but it differs from the relations (14), (16) and (17) in the method of derivation: the relation (18) was obtained by measuring the transfer of energy from wind to waves by the working of air-pressure fluctuations on the moving water surface, but the relations (14), (16) and (17) were obtained by measuring the growth of wave energy induced by the wind. Therefore, if other mechanisms exist that transfer the energy effectively from wind to waves, and if the energy dissipation in the wave field is smaller than the transferred energy,

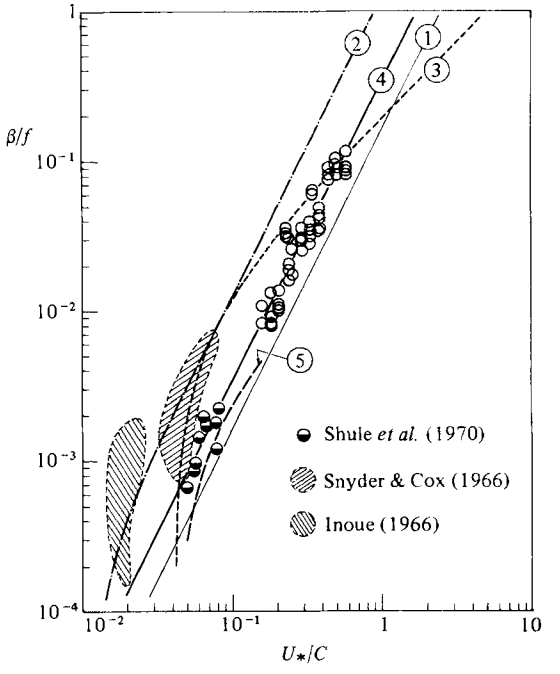

FIGURE 12. Comparison of various relations for the growth rate. Curves show theoretical and empirical relations of (1) Miles (1959), (2) Inoue (1966), (3) Snyder & Cox (1966), (4) equation (14), (5) Snyder *et al.* (1981).

the growth rate determined from the wave energy should be larger than that determined from the wave-induced pressure. Furthermore, the growth rates of Snyder & Cox (1966) and Inoue (1966) would be affected by the nonlinear wave–wave interaction, because their growth rates were determined from spectral data of ocean waves.

Quite recently Plant (1982) obtained an empirical relation

$$\beta = \frac{[(0{\cdot}04 \pm 0{\cdot}02)\, U_*^2\, \omega \cos\theta]}{C^2} \tag{19}$$

for the growth rate β by using recently published data taken in wind-wave tanks and on the ocean. Here θ is the angle between wind and waves. For $\theta = 0$, (19) reduces to

$$\frac{\beta}{f} = (0{\cdot}25 \pm 0{\cdot}13)\left(\frac{U_*}{C}\right)^2. \tag{20}$$

Our present relation (14) is quite similar to (20) from Plant (1982), though the former gives values near the upper bound of the latter within its error bars.

4.5. *The effect of the surfactant on the growth of the regular waves by the wind*

The growth of the regular waves by the wind was measured on water containing the surfactant (sodium lauryl sulphate, concentration $2{\cdot}6 \times 10^{-2}$ %). Typical records of waves measured at fetches $X = 0, 3, 6, 9$ (m) for wind speed $U_r = 10$ m/s, are shown in figure 13, which corresponds to figure 5, the records of the same waves measured on the pure water for the same wind speed. The upper record shows the surface

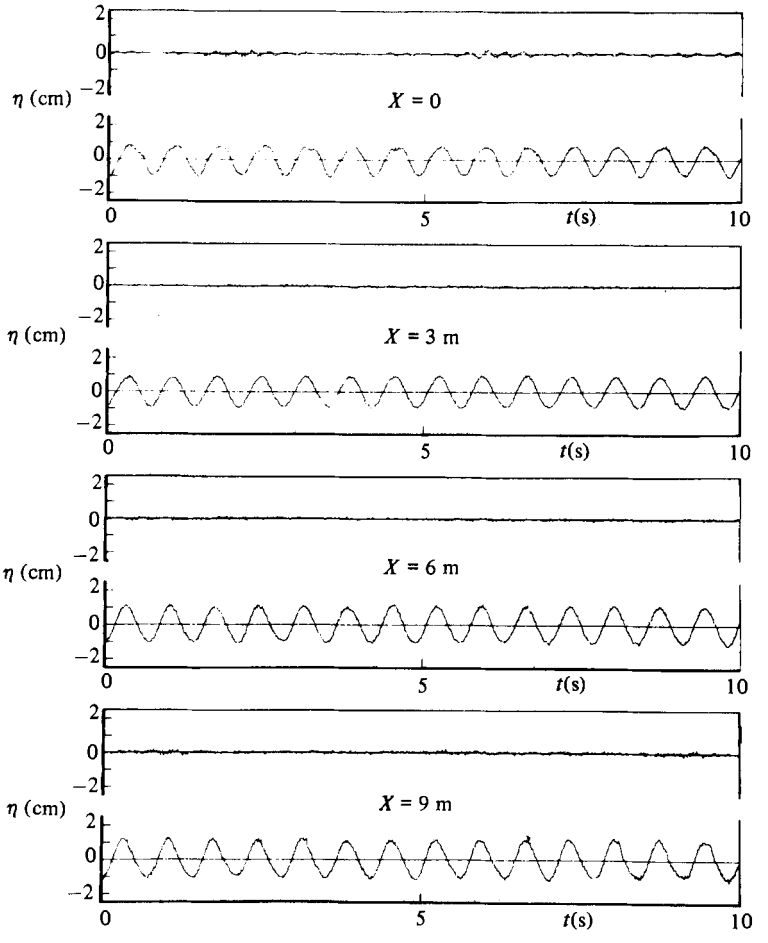

FIGURE 13. The same as figure 5 except for water containing surfactant ($2{\cdot}6 \times 10^{-2}$ %).

fluctuation by the wind in the absence of the regular waves, and the lower record shows the regular waves under the wind action. Figure 13 shows that wind waves do not develop on the surface of regular waves or on the still water surface.

Figure 14 shows the wave spectra corresponding to the wave records shown in figure 13, though the spectra at all stations, fetches $X = 0, 1, 2, \ldots, 10$ (m), are shown in this figure. The first spike corresponds to the fundamental frequency component of the regular waves. As expected from the wave records (figure 13) no wind-wave spectra are seen in figure 14.

The growth rate β of the fundamental frequency component of the regular waves was determined in a similar way as in the experiment for pure water. The dimensionless growth rate β/f for the regular waves on the water containing the surfactant was compared in figure 15 with that for the waves on pure water. In figure 15 individual data of β/f for both cases are shown as a function of the dimensionless friction velocity U_*/C without showing the difference of $(H/L)_0$. It is very interesting that the relation between β/f and U_*/C is not much affected by the surfactant, if the measured friction velocity of the wind is used in the relation.

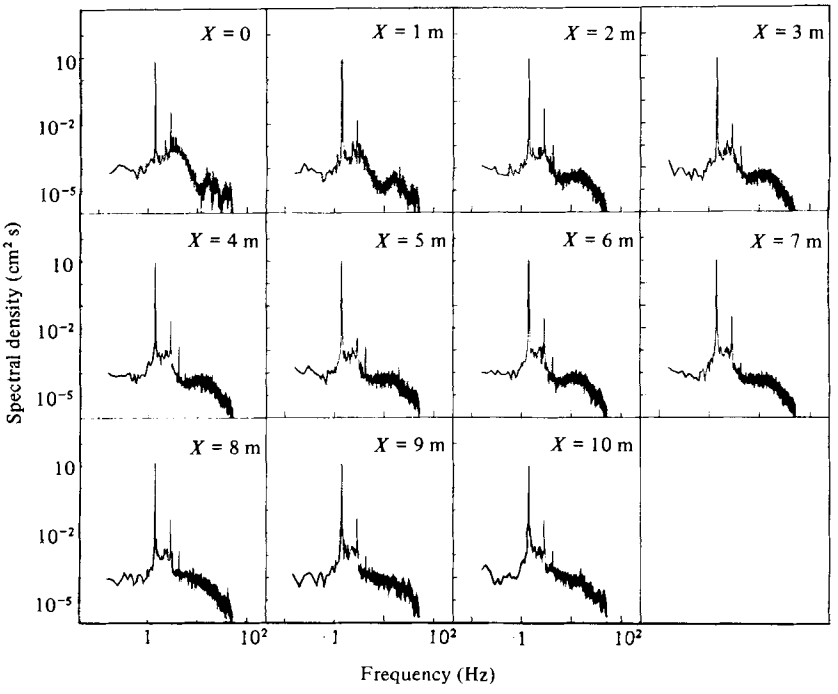

FIGURE 14. Growth of the wave spectrum for water containing surfactant ($2{\cdot}6 \times 10^{-2}$%).

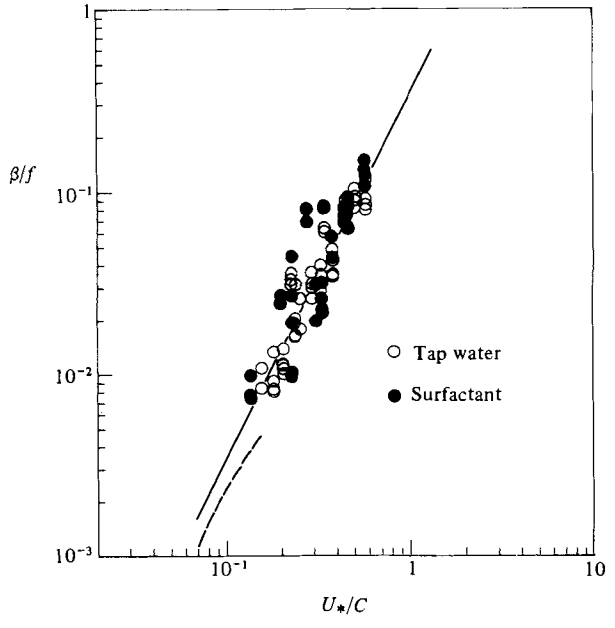

FIGURE 15. Comparison of β/f for tap water with that for water containing surfactant ($2{\cdot}6 \times 10^{-2}$%). The curves are the same as in figure 11.

5. Conclusion

Growth of mechanically generated water waves under wind action was measured for a wide range of experimental conditions. Almost the same measurements were made for pure water and for water containing the surfactant. In the latter case no wind waves were generated for wind speeds up to $U_{10} \approx 15$ m/s. Therefore, we can examine the growth of the mechanically generated waves under the wind action without the effects of co-existing short wind waves. Before the wave-growth experiment, attenuation of the mechanically generated waves was measured for both cases in the absence of wind.

The mechanically generated waves attenuated exponentially with distance x for both cases. Measured damping coefficients of the waves were very close to those predicted by taking account of the viscous energy dissipations at the water surface, the sidewalls and the bottom of the flume. The measured and predicted damping coefficients for the waves on water containing surfactant were larger than those for the waves on pure water, which could be attributed to the effect of the surface film of the surfactant.

The mechanically generated waves under wind action grew exponentially with fetch for both cases. The measured growth rate of the waves on pure water shows a quadratic relation (14) to the friction velocity of the wind, which is similar to the relation obtained recently by Plant (1982). The same relation holds approximately for the waves on water containing surfactant if the measured friction velocity of the wind was used for the relation.

The most interesting finding of this study can be expressed as follows: the growth of the regular waves by the wind is uniquely related to the friction velocity of the wind, and the effect of the overlapping wind waves on the growth of the regular waves appears through the change of the friction velocity of the wind.

The authors are indebted to Dr A. Masuda for his helpful discussions and to two referees for their invaluable comments. They also wish to express their gratitudes to Mr K. Marubayashi and Mr M. Ishibashi for their assistance in the laboratory experiment, and to Miss M. Hojo for typing the manuscript.

This study was partially supported by the Grant-in-Aid for Scientific Research, Project no. 302037 by the Ministry of Education.

REFERENCES

Bole, J. B. & Hsu, E. Y. 1969 Response of gravity water waves to wind excitation. *J. Fluid Mech.* **35**, 657–675.

Dobson, F. W. 1971 Measurements of atmospheric pressure on wind-generated sea waves. *J. Fluid Mech.* **48**, 91–127.

Elliot, J. A. 1972 Microscale pressure fluctuations near waves being generated by the wind. *J. Fluid Mech.* **54**, 427–448.

Garrett, C. & Smith, J. 1976 On the interaction between long and short surface waves. *J. Phys. Oceanogr.* **6**, 926–930.

Gottifredi, J. C. & Jameson, G. J. 1970 The growth of short waves on liquid surfaces under the action of a wind. *Proc. R. Soc. Lond.* A **319**, 373–397.

Hasselmann, K. 1968 Weak interaction theory of ocean surface waves. In *Basic Developments in Fluid Mechanics* (ed. M. Holt), vol. 2. pp. 117–182. Academic.

Hasselmann, K. 1971 On the mass and momentum transfer between short gravity waves and large-scale motions. *J. Fluid Mech.* **50**, 189–205.

HATORI, M., TOKUDA, M. & TOBA, Y. 1981 Experimental study on strong interaction between regular waves and wind waves (1). *J. Oceanogr. Soc. Japan* **37**, 111–119.

HUNT, J. N. 1952 Viscous damping of waves over an inclined bed in a channel of finite width. *Houille Blanche* **7**, 836–842.

INOUE, T. 1966 On the growth of the spectrum of a wind generated sea according to a modified Miles–Phillips mechanism and its application to wave forecasting. *New York Univ. Geophys. Sci. Lab. Rep.* TR67–5.

LAMB, H. 1932 *Hydrodynamics.* Cambridge University Press.

LONGUET-HIGGINS, M. S. 1969 A nonlinear mechanism for the generation of sea waves. *Proc. R. Soc. Lond.* A **311**, 371–389.

MILES, J. W. 1959 On the generation of surface waves by shear flows. Part 2. *J. Fluid Mech.* **6**, 568–582.

MILES, J. W. 1962 On the generation of surface waves by shear flows. Part 4. *J. Fluid Mech.* **13**, 433–448.

MITSUYASU, H. 1966 Interaction between water waves and wind (1). *Rep. Res. Inst. Appl. Mech., Kyushu Univ.* **14**, 67–88.

MITSUYASU, H. & HONDA, T. 1982 The effects of surfactant on certain air-sea interaction phenomena. In *Proc. IUCRM Symp. on Wave Dynamics and Radio Probing of the Ocean Surface.* (In press).

MIZUNO, S. 1975 Growth of mechanically generated waves under a following wind (1). *Rep. Res. Inst. Appl. Mech., Kyushu Univ.* **22**, 357–376.

PHILLIPS, O. M. 1963 On the attenuation of long gravity waves by short breaking waves. *J. Fluid Mech.* **16**, 321–332.

PHILLIPS, O. M. & BANNER, M. L. 1974 Wave breaking in the presence of wind drift and swell. *J. Fluid Mech.* **66**, 625–640.

PLANT, W. J. 1982 A relationship between wind stress and wave slope. *J. Geophys. Res.* **87**, 1961–1967.

SCHULE, J. J., SIMPSON, Z. S. & DELEONIBUS, P. S. 1971 A study of fetch-limited wave spectra with an airborne laser. *J. Geophys. Res.* **76**, 4160–4171.

SNYDER, R. L. & COX, C. S. 1966 A field study of the wind generation of ocean waves. *J. Mar. Res.* **24**, 141–178.

SNYDER, R. L., DOBSON, F. W., ELLIOTT, J. A. & LONG, R. B. 1981 Array measurements of atmospheric pressure fluctuations above surface gravity waves. *J. Fluid Mech.* **102**, 1–59.

VALENZUELA, G. R. & WRIGHT, J. W. 1976 The growth of waves by modulated wind stress. *J. Geophys. Res.* **81**, 5795–5796.

WILSON, W. S., BANNER, M. L., FLOWER, R. J., MICHAEL, J. A. & WILSON, D. G. 1973 Wind-induced growth of mechanically generated water waves. *J. Fluid Mech.* **58**, 435–460.